Polar Meteorol. Glaciol., **19**, 15–27, 2005
© 2005 National Institute of Polar Research

Spreading of Antarctic Bottom Water examined using the CFC-11 distribution simulated by an eddy-resolving OGCM

Yoshikazu Sasai[1]*, Akio Ishida[1,2], Hideharu Sasaki[3], Shintaro Kawahara[3], Hitoshi Uehara[3] and Yasuhiro Yamanaka[1,4]

[1]*Frontier Research Center for Global Change, Japan Agency for Marine-Earth Science and Technology, 3173–25, Showa-machi, Yokohama 236-0001*
[2]*Institute of Observational Research for Global Change, Japan Agency for Marine-Earth Science and Technology, Yokosuka 237-0061*
[3]*Earth Simulator Center, Japan Agency for Marine-Earth Science and Technology, Yokohama 236-0001*
[4]*Graduate School of Environmental Science, Hokkaido University, Sapporo 060-0810*
**Corresponding author. E-mail: ysasai@jamstec.go.jp*

(Received February 25, 2005; Accepted July 11, 2005)

Abstract: We have investigated the spreading and pathway of Antarctic Bottom Water (AABW) using the simulated distribution of chlorofluorocarbons (CFCs) in a global eddy-resolving (1/10°) OGCM. Our goal is understanding of the processes and pathways determining the distribution of CFCs in the Southern Ocean, where much of this tracer is entrained by formation of deep and bottom water. The simulated high CFC-11 water reveals the newly formed AABW around the Antarctic Continent. The main source regions of AABW in the model are in the Weddell Sea (60°–30°W), offshore of Wilkes Land (120°–160°E) and in the Ross Sea (170°E–160°W). In our model, spreading of simulated CFC-11 in the deep Southern Ocean from the newly formed AABW regions is more similar to the observed distribution than in coarse-resolution models. In the Weddell Sea, the high CFC-11 water spreads eastward with the Antarctic Circumpolar Current (ACC) and flows northward to the Argentine Basin. The high CFC-11 water from Wilkes Land joins with the high CFC-11 water from the Ross Sea. Some of the high CFC-11 water from Wilkes Land flows northward toward New Zealand. The high CFC-11 water from the Ross Sea flows eastward with the ACC along the Mid Ocean Ridge and northward to the Southeast Pacific Basin.

key words: AABW, CFC-11, Southern Ocean, Eddy-resolving OGCM

1. Introduction

Chlorofluorocarbons (CFCs) have been widely used to study oceanic circulation, mixing processes, ventilation, and water mass formation processes (*e.g.*, Doney and Bullister, 1992; Warner and Weiss, 1992; Watanabe *et al*., 1994). In high latitudes, CFCs absorbed in the surface ocean are directly carried to deeper layers through density-driven thermohaline circulation. During deep-water formation, atmospheric constituents such as CFCs are introduced into newly formed water. The measured CFCs in the ocean are used to investigate the ocean circulation in high latitudes (*e.g.*,

Haine *et al*., 1998; Orsi *et al*., 1999; Smethie *et al*., 2000; Klatt *et al*., 2002).

One of the major deep and bottom water sources to the open oceans is near the Antarctic continental margins. Orsi *et al*. (1999) described the large-scale patterns of the Southern Ocean bottom water circulation using the World Ocean Circulation Experiment (WOCE) hydrographical CFC data. They also estimated from the CFC inventories that the production rate of Antarctic Bottom Water (AABW) is about 8 Sv ($1\,\mathrm{Sv} = 10^6\,\mathrm{m^3\,s^{-1}}$). Haine *et al*. (1998) used CFC measurements to estimate the mean speed and mixing rate of the abyssal flow at several observed section in the Southern and southwestern Indian Oceans using simple kinematic circulation models. The transit time is 23 ± 5 years from the Weddell Sea to the Crozet-Kerguelen Gap. Repeated observations of CFC were used to estimate mean ages for the deep water along the Greenwich Meridian in the Weddell Sea (Klatt *et al*., 2002). The ages are between 3 and 19 years.

Observed CFCs are used as a reference to assess the skill of ocean circulation models that are used to simulate the uptake and redistribution of anthropogenic CO_2 in the oceans (*e.g*., England, 1995; England and Hirst, 1997). Dutay *et al*. (2002) compared simulated CFC-11 in the 13 coarse resolution models that participated in the Ocean Carbon-cycle Model Intercomparison Project (OCMIP-2). In the Southern Ocean, these models show a wide range of estimates for simulated CFC-11 inventory because of different deep-water ventilation. For the AJAX CFC-11 section along the Greenwich Meridian, the models with explicit formulations for isopycnal diffusion and the Gent and McWilliams parameterization (Gent and McWilliams, 1990) produce steeper, more realistic ventilation of Subantarctic Mode Water (SAMW). However, these coarse-resolution models typically underestimate CFC-11 concentrations in the deep layer ventilated by the AABW.

Currently, high-resolution ocean models are used for tracer simulations (Beismann and Redler, 2003; Sen Gupta and England, 2004; Sasai *et al*., 2004). The horizontal grid spacing is from $1/3^\circ$ (eddy-permitting) to $1/10^\circ$ (eddy-resolving). Beismann and Redler (2003) discussed the influence of parameterization for air-sea gas exchange and subgrid-scale processes on the rate at which CFC-11 enters the North Atlantic Ocean and its dependence on horizontal resolution from medium ($4/3^\circ$) to eddy-permitting ($1/3^\circ$). Sen Gupta and England (2004) have developed an offline tracer transport model run at an eddy-permitting ($1/4^\circ$) resolution to investigate interior ventilation pathways on interdecadal to intercentennial timescales. The formation of bottom water around the Antarctic margins is also generally too weak because the offline model is lacking realistic interior ocean convective overturning and down-slope flows, although there is excellent qualitative agreement with observations in the Weddell and Ross Seas. A first CFC-11 simulation using a global eddy-resolving ($1/10^\circ$) ocean general circulation model has been presented by Sasai *et al*. (2004). The model reproduced well the section along the Greenwich Meridian (AJAX) and 170°W (WOCE P15S). The simulated CFC-11 inventory along these two sections is very similar to the observed. In the South Atlantic, the model indicates two pathways transporting CFC-11 from the Weddell Sea to the AJAX section. In this study, we describe in detail the pathways and spreading of newly formed AABW from the Antarctic Continent, including the Weddell and Ross Seas. We also estimate the CFC apparent age and spreading rate of newly

formed AABW in the Southern Ocean.

2. Ocean model and CFC-11 forcing

The ocean model used in this study is an eddy-resolving model incorporating equations for simulating CFC-11 in the OGCM for the Earth Simulator (OFES) (Masumoto *et al*., 2004), which is based on the Geophysical Fluid Dynamics Laboratory's Modular Ocean Model (MOM3) (Pacanowski and Griffies, 2000). The domain covers from 75°S to 75°N. The horizontal grid spacing is 1/10°. The model has 54 vertical levels, with varying distance between the levels from 5 m at the surface to 330 m at the maximum depth of 6065 m. The model topography is constructed from the 1/30° bathymetry dataset created by the OCCAM Project at the Southampton Oceanography Centre. The model bathymetry in the Southern Ocean is shown in Fig. 1.

Monthly mean wind stresses averaged from 1950 to 1999 from the National Centers for Environmental Prediction/National Center for Atmospheric Research NCEP/NCAR reanalysis data are used for the climatological integration. The surface heat flux is calculated by the bulk formula of Rosati and Miyakoda (1988), using monthly mean values of NCEP/NCAR reanalysis data. Surface salinity is restored to the

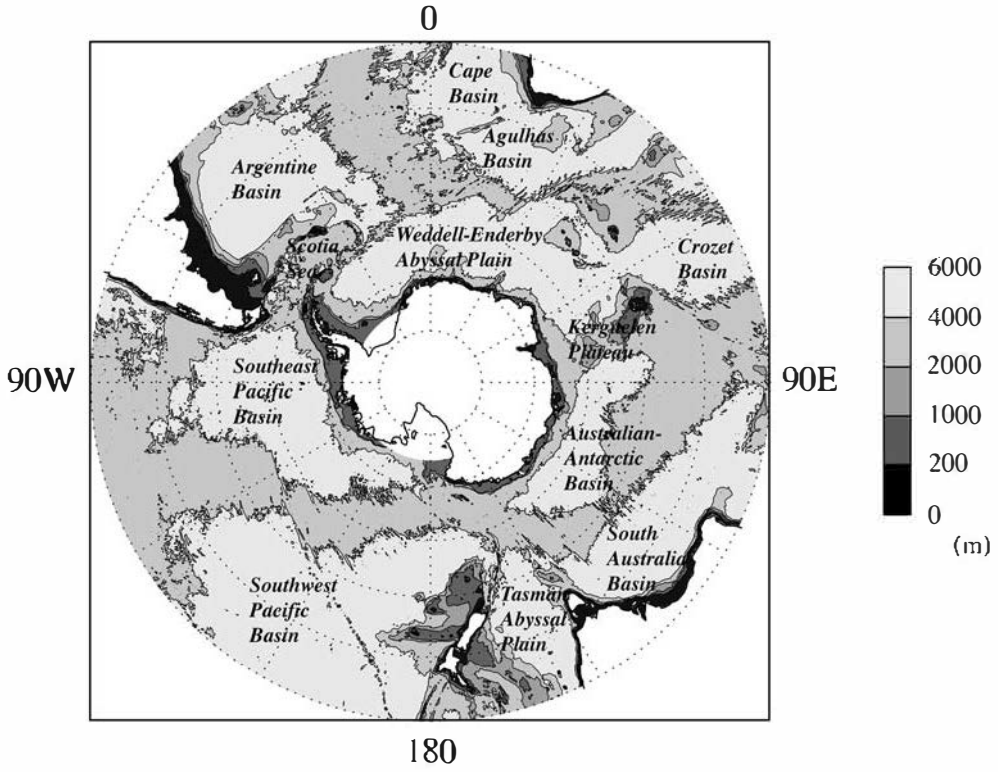

Fig. 1. Model topography in the Southern Ocean. The contour intervals are 200, 1000, 2000 and 4000 m depth.

monthly mean climatological values (World Ocean Atlas 1998, WOA98). In the near polar region (72°–75°), temperature and salinity are restored throughout the water column. The restoring time-scale is set to 1 day at 75°. The model is integrated for 50 years from the annual mean temperature and salinity fields (WOA98) without motion (Masumoto *et al*., 2004).

The simulation of CFC-11 is performed according to OCMIP-2 protocol (Dutay *et al*., 2002). Air-sea CFC flux, F_{CFC}, is calculated by the following equation

$$F_{CFC}=K_W(\alpha C_{atm}-C_{sea}), \quad (1)$$

where K_W is the gas transfer velocity, α is the solubility of CFC-11 in seawater, C_{atm} is the partial pressure of CFC-11 in dry air, and C_{sea} is the modeled CFC-11 concentration at the sea surface. The gas transfer velocity, K_W, is a function of the wind velocity, the Schmidt number of gas (Wanninkof, 1992) and the fraction of the sea surface covered with ice (Walsh, 1978; Zwally *et al*., 1983). The solubility of CFC-11 in seawater, α, is computed using modeled sea surface temperature and salinity (Warner and Weiss, 1985). C_{atm} is assumed to be uniform in each hemisphere, with temporal values from the reconstructed annual mean mole fraction of CFC-11 at 41°S and 45°N (Fig. 2) (Walker *et al*., 2000). Between 10°S to 10°N, we made a linear transition between the two hemispheres.

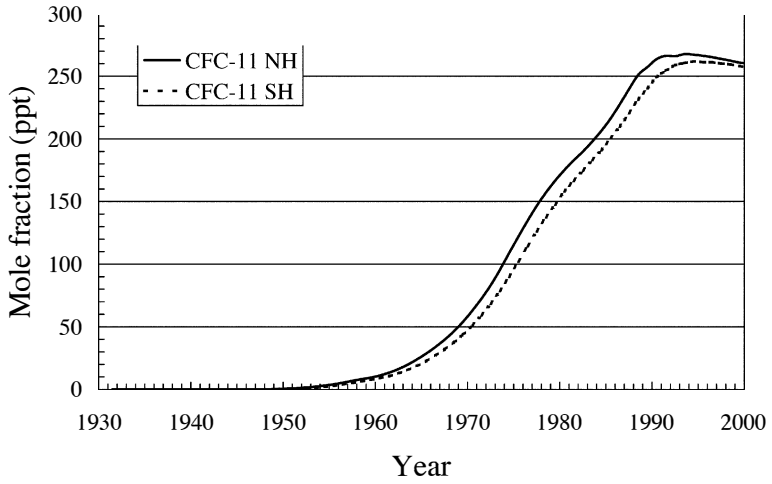

Fig. 2. Temporal evolution of the atmospheric CFC-11 mole fraction in both hemispheres (Walker et al., 2000). Solid line is in the northern hemisphere and dashed line is in the southern hemisphere.

The 50-year integration was performed before starting the CFC-11 simulation. The initial CFC-11 concentration was set to zero in the whole model domain. The CFC-11 experiment was performed from 1950 until the end of 1997.

3. Results

To assess the performance of this high resolution OGCM, means of potential temperature and salinity at the bottom layer over the last 20 years of simulation are shown in Fig. 3. AABW has been observed in the Weddell Sea, the Amery Basin, offshore of the Adélie Coast, and in the Ross Sea (*e.g.*, Jacobs *et al.*, 1970; Gill, 1973; Rintoul and Bullister, 1999). In the Weddell Sea, the bottom water appears with potential temperature <-0.8°C and salinity <34.66 PSU (Figs. 3a and 3c). The simulated bottom temperature and salinity are close to the data (WOA98). In the Ross Sea, the bottom water is saltier than that in the Weddell Sea (Fig. 3c; salinity >34.80 PSU). The model reproduces the high salinity water in the western Ross Sea (Fig. 3d). AABW is formed in both the Weddell and Ross Seas in the model. The bottom temperature around the Antarctic Continent is colder than the observed by 0.2°C in the model. The simulated cold temperature at the bottom indicates that the model reproduce the production of the bottom water.

Figure 4 shows the temporal evolution of bottom CFC-11 concentration in the

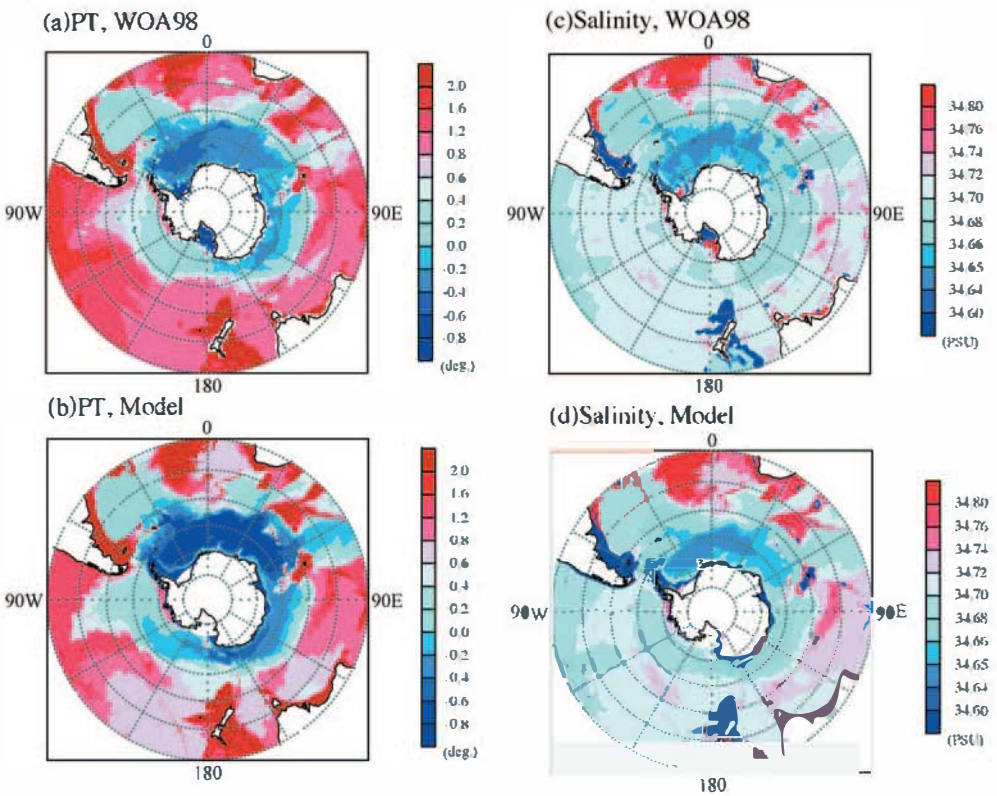

Fig. 3. Comparisons of bottom potential temperature (°C) from (a) WOA98 and (b) model and salinity (PSU) from (c) WOA98 and (d) model in the Southern Ocean. Simulated (b) potential temperature and (d) salinity are averaged for the last two decades.

model from 1950 to 1997 to investigate the pathway and spreading of the newly formed AABW around the Antarctic Continent. At the beginning of the simulation (Fig. 4a), the high CFC-11 water does not reach the bottom layer. After integration for 10 years, the high CFC-11 water begins to spread around the Antarctic Continent in 1960 (Fig. 4b). In the model, AABW is formed in the Weddell Sea (60°–30°W), offshore of Wilkes Land (120°–160°E), and in the Ross Sea (170°E–160°W). Newly formed

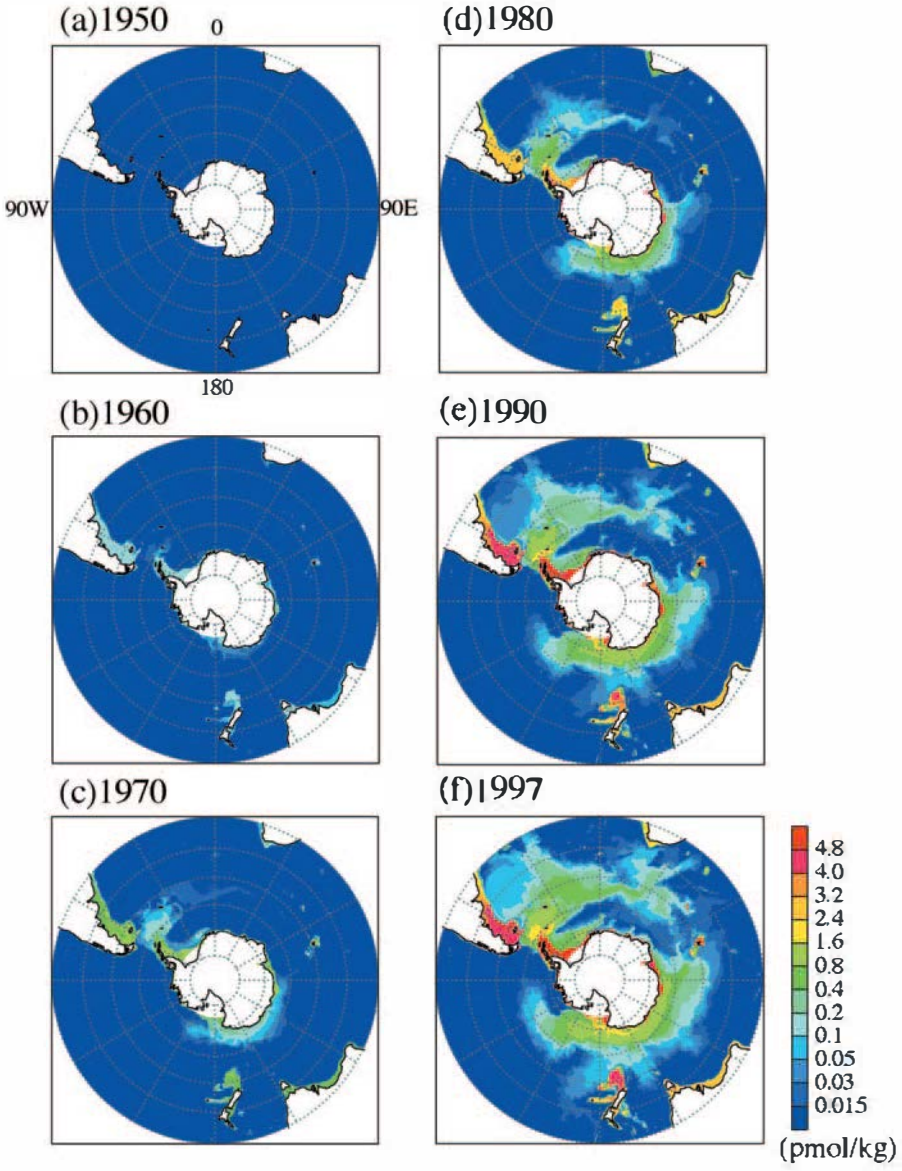

Fig. 4. Temporal variation of annual mean simulated CFC-11 concentration (pmol kg^{-1}) in the bottom layer from 1950 to 1997.

AABW in the Weddell Sea first spreads northward along the Antarctic Peninsula, across the South Scotia Ridge (Locarnini *et al*., 1993; Whitworth *et al*., 1994), and into the South Scotia Sea. From there it flows into the Georgia Basin and is transported eastward with the ACC to the southwest Indian Ocean and northward to the Argentine Basin (Fig. 4d). In the model, newly formed AABW in the Ross Sea spreads on the bottom slope and divides into two directions on the Mid Ocean Ridge along 180°. Some of the AABW formed in the Ross Sea flows eastward with the ACC to the Southeast Pacific Basin, some flows westward along the Antarctic Continent to the Kerguelen Plateau (Figs. 4e and 4f). The latter flows northward along the Kerguelen Plateau to the Crozet Basin (Fig. 4f). The pattern of simulated CFC-11 distribution is more similar to the observed pattern (Orsi *et al*., 1999) than are those from coarse-resolution models (Dutay *et al*., 2002) and a previous high-resolution (1/4°) model (Sen Gupta and England, 2004). In particular, the spreading of high CFC-11 water from the Weddell and Ross Seas is very similar to the observed pattern. In the Amery Basin (50°–100°E), however, the CFC-11 concentrations at the bottom are lower than the observed values (Orsi *et al*., 1999). The model does not produce AABW along the Antarctic coast except in the Weddell and Ross Seas. The restoring condition is applied only in these regions because temperature and salinity is restored to WOA98 south of 72°S.

The distribution of *p*CFC-11 apparent age (in years) in the bottom layer is shown in Fig. 5. The *p*CFC-11 apparent age can be calculated from the partial pressure of

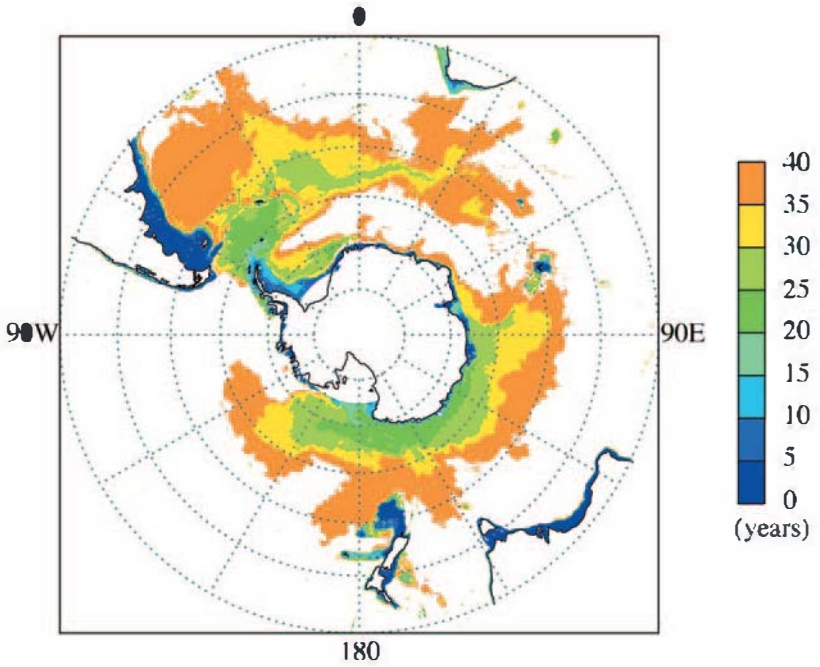

Fig. 5. The pCFC-11 apparent age (in years) in the bottom layer. The pCFC-11 apparent age is calculated based on the atmospheric pCFC-11 (Walker et al., 2000) at the reference year (1990).

dissolved CFC-11. The *p*CFC-11 apparent age for water can be obtained directly by comparing the *p*CFC-11 to the atmospheric history (Fig. 2). The reference year is set to 1990, which corresponds to zero age. The estimated date indicates the elapsed time since a surface water mass was last in contact with the atmosphere. The *p*CFC-11 apparent ages are younger than 20 years around the Antarctic Continent, especially in the Weddell and Ross Seas. The CFC-11 concentrations at the bottom in 1990 are so high (Fig. 4e) because the newly formed bottom water was recently in contact with the atmosphere. The *p*CFC-11 apparent age increases from the Weddell and Ross Seas to the Argentine Basin, the Agulhas Basin, the Kerguelen Plateau and the Southeast Pacific Basin, corresponding to the decrease of CFC-11 concentration (Fig. 4). AABW formed in the Weddell Sea flows into the South Scotia Sea (20–25 years), and spreads eastward to the Agulhas Basin (30–40 years) and northward to the Argentine Basin (30–40 years). Some of the AABW formed in the Ross Sea flows eastward to the Southeast Pacific Basin (30–40 years) and westward along the Antarctic Continent (20–25 years) to the Kerguelen Plateau (35–40 years). At low CFC-11 concentration, dilution will bias the *p*CFC-11 apparent ages toward older values. Therefore, our estimates may be too old.

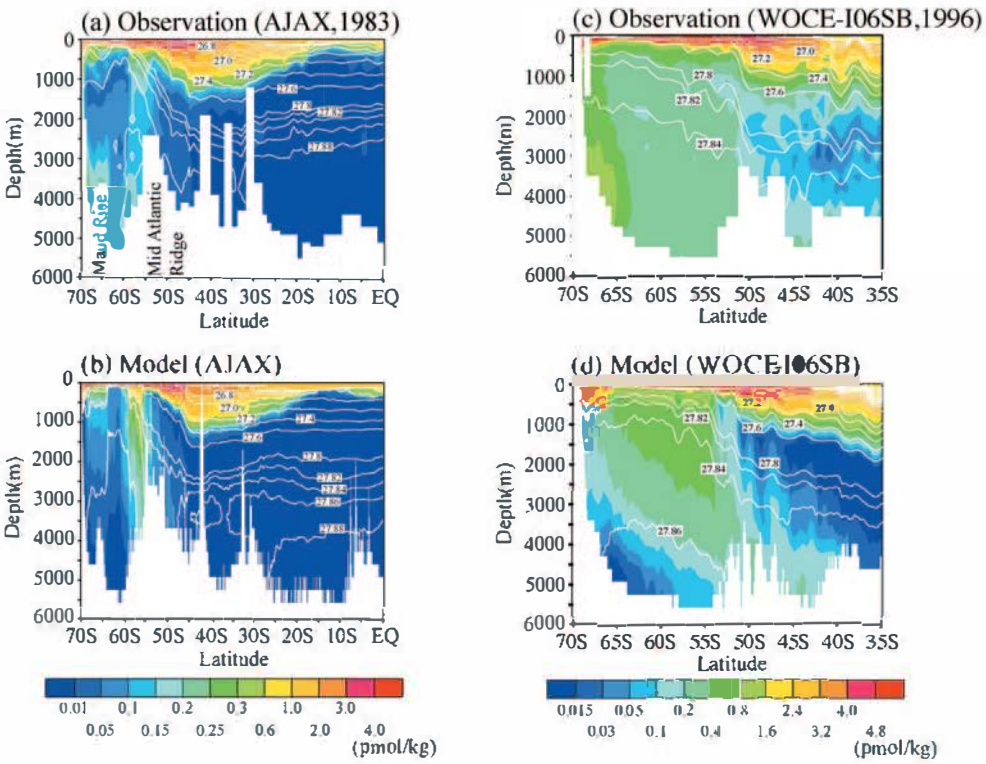

Fig. 6. Comparison of the CFC-11 concentrations (pmol kg^{-1}) from observations and model with the potential density (solid lines) along (a)–(b) 0°E in the South Atlantic (1983), (c)–(d) 30°E in the South Indian (1996).

The Weddell and Ross Seas are two large source regions of AABW in the Southern Ocean. The AJAX section in the South Atlantic Ocean along the Greenwich Meridian (Warner and Weiss, 1992), and the WOCE I06SB section along 30°E (WOCE Data Products Committee, 2000) in the South Indian Ocean show spreading of AABW from the Weddell Sea (Fig. 6). The WOCE P15S section along 170°W in the South Pacific Ocean, and the WOCE I09S section along 115°E in the South Indian Ocean show spreading from the Ross Sea (Fig. 7). The distributions along these four sections are well reproduced. In the upper layer, high CFC-11 water penetrates to 1000 m depth at 50°S by the Subantarctic Mode Water (SAMW) ventilation for each section. Along the AJAX section, the observed CFC-11 (Fig. 6a) reveals two maxima at the slope of the Mid-Atlantic Ridge and the Antarctic Continent in the bottom layer. The observed CFC-11 maximum at the Antarctic Continent increases with time as the deep water flows from the Amery Basin (east side of the Weddell Sea) (Klatt *et al*., 2002). The simulated CFC-11 concentrations (Fig. 6b) are less than the observed (Fig. 6a) because the model does not produce deep water in the Amery Basin. The observed CFC-11 maximum (Fig. 6a) at the Mid-Atlantic Ridge is well reproduced in the model (Fig. 6b).

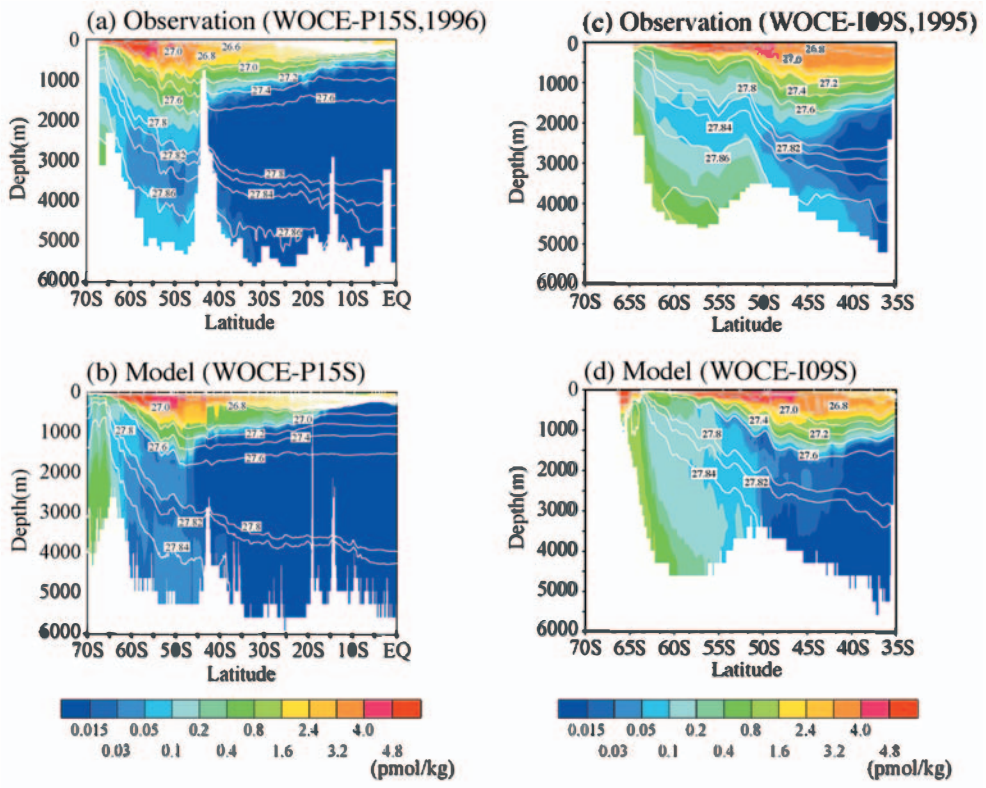

Fig. 7. Comparison of the CFC-11 concentrations (pmol kg^{-1}) from observations and model with the potential density (solid lines) along (a)–(b) 170°W in the South Pacific (1996), and (c)–(d) 115°E in the South Indian (1995).

Along the WOCE I06SB section, the observed CFC-11 peaks at the slope of the Antarctic Continent (3000–5000 m) and higher CFC-11 concentrations extend from 1000 m to the bottom between 50°S and 65°S (Fig. 6c). The observed CFC-11 maximum at the slope of the Antarctic Continent is the result of flow from the Amery Basin (Klatt *et al*., 2002). The simulated CFC-11 concentrations are lower than the observed because the high CFC-11 water does not extend far enough down the slope. The simulated CFC-11 concentrations from 1000 m to 3000 m between 50°S and 65°S (Fig. 6d) are much higher than the observed. In the model, high CFC-11 water from the Weddell Sea does not penetrate to the ocean floor. Although the CFC-11 concentration is higher than the observed, the pathway from the Weddell Sea to the southwest Indian Ocean has been reported based on the observed CFCs (Haine *et al*., 1998). Along the WOCE P15S and I09S sections (Figs. 7a and 7c), CFC-11 concentration is high at the slope of the Antarctic Continent from the surface to the bottom layer. The pattern of simulated CFC-11 distributions (Figs. 7b and 7d) in the bottom layer is well reproduced.

Figure 8 shows a three-dimensional view of simulated CFC-11 distributions in the Weddell Sea and the Ross Sea. This view clearly shows the simulated pathways and spreading of high CFC-11 water from the AABW formation regions. In the Weddell

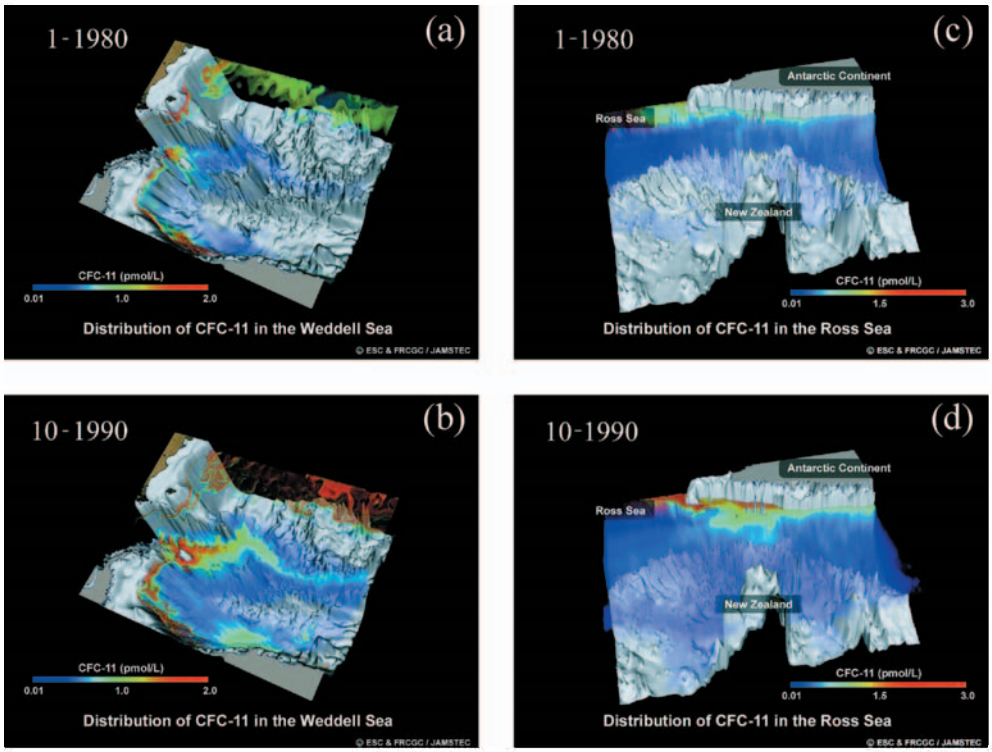

Fig. 8. Monthly mean distribution of CFC-11 concentration (pmol l^{-1}) in the (a)–(b) Weddell Sea and (c)–(d) Ross Sea.

Sea (Figs. 8a and 8b), AABW is formed along the western boundary coast of the Weddell Sea. The formed AABW flows over the South Scotia Ridge, and into the Scotia Sea to the AJAX section. Some of the formed AABW flows eastward along the South Scotia Ridge. In the Ross Sea (Figs. 8c and 8d), AABW is formed in the eastern Ross Sea. The formed AABW extends to the boundary of the Mid-Ocean Ridge. The high CFC-11 water passes through the narrow passage of the Mid-Ocean Ridge and spreads northward toward near New Zealand. The high CFC-11 water branches into two pathways off New Zealand.

4. Summary

Using a global eddy-resolving OGCM, we investigated the spreading and pathways of AABW with the simulated CFC-11 distribution. The model reproduces the CFC-11 distribution in the deep layer due to ventilation of the AABW from the Weddell and Ross Seas. The model indicates the pathways of CFC-11 spreading from the Weddell Sea to the southwestern Indian Ocean (WOCE I06SB section). The spreading ages of newly formed AABW from the Weddell and Ross Seas are about 40 years based on the *p*CFC-11 apparent ages. The AABW in the Argentine Basin, Agulhas Basin, Kerguelen Plateau, and Southwest Basin, was formed 40 years ago in the Weddell and Ross Seas. The pathways of CFC-11 from the Ross Sea in the model are westward along the Antarctic Continent to the Indian Ocean and eastward with the ACC along the Mid-Ocean Ridge.

The eddy-resolving ($1/10^{\circ}$) model represents the complex bottom topography and the boundary currents along the bottom topography. Low-resolution models (*e.g.*, Dutay *et al*., 2002) depend on parameterizations for sub-grid scale mixing and convection to produce a realistic spatial distribution of recently formed AABW in the Southern Ocean. An eddy-permitting ($1/4^{\circ}$) model (Sen Gupta and England, 2004) improved the interior ocean ventilation pathways of CFC. However, because the offline model lacked realistic interior ocean convective overturning and down-slope flows, CFC concentrations around the Antarctic margin were generally lower than observed. Convection processes affecting tracers are explicitly simulated in our online model. Also, sub-grid scale mixing need not be parameterized in the high-resolution models. Owing to these advantages, realistic spreading and pathways of CFC-11 due to AABW ventilation is represented in our model. However, CFC-11 concentrations at the bottom in the Amery Basin are less than observed. The AABW formation does not extend far enough down the Antarctic continental slope because the model does not include sea-ice process. Dutay *et al*. (2002) revealed that ocean models coupled with a sea-ice model systematically provided more realistic patterns of AABW formation, than those without this component. Doney and Hecht (2002) also found that the surface boundary conditions in permanently sea-ice-covered regions are a major factor causing underestimation of formation of dense, cold, and relatively saline shelf waters, the precursors of AABW. In the Southern Ocean, shelf-edge processes play a major role in the formation of deep and bottom waters (Foster and Carmack, 1976). Including the sea-ice model and freshwater fluxes are necessary conditions for producing a realistic distribution of AABW formation regions.

Acknowledgments

We thank Drs. Y. Masumoto, T. Kagimoto, Y. Tsuda, M. Kanazawa, and S. Kitawaki for their efforts to develop the OFES on the Earth Simulator.

References

Beismann, J.-O. and Redler, R. (2003): Model simulations of CFC uptake in North Atlantic Deep Water: Effects of parameterizations and grid resolution. J. Geophys. Res., **108**, 3159, doi: 10.1029/2001JC001253.

Doney, S.C. and Bullister, J.L. (1992): A chlorofluorocarbon section in the eastern North Atlantic. Deep Sea Res., **39**, 1857–1883.

Doney, S.C. and Hecht, M. (2002): Antarctic bottom water formation and deep-water chlorofluorocarbon distribution in a global ocean climate model. J. Phys. Oceanogr., **32**, 1642–1666.

Dutay, J.-C., Bullister, J.L., Doney, S.C., Orr, J.C., Najjar, R. and other 23 authors (2002): Evaluation of ocean model ventilation with CFC11: comparison of 13 global ocean models. Ocean Modeling, **4**, 89–120.

England, M.H. (1995): Using chlorofluorocarbons to assess ocean climate models. Geophys. Res. Lett., **22**, 3051–3054.

England, M.H. and Hirst, A.C. (1997): Chlorofluorocarbon uptake in a World Ocean model 2. Sensitivity to surface thermohaline forcing and subsurface mixing parameterizations. J. Geophys. Res., **102**, 15709–15731.

Foster, T.D. and Carmack, E.C. (1976) Frontal zone mixing and Antarctic Bottom Water formation in the southern Weddell Sea. Deep-Sea Res., **23**, 301–317.

Gent, P.R. and McWilliams, J.C. (1990): Isopycnal mixing in ocean circulation models. J. Phys. Oceanogr., **20**, 150–155.

Gill, A.E. (1973): Circulation and bottom water formation in the Weddell Sea. Deep-Sea Res., **20**, 111–140.

Haine, T.W.N., Watson, A.J., Liddicoat, M.L. and Dickson, R.R. (1998): The flow of Antarctic Bottom Water to the southwest Indian Ocean estimated using CFCs. J. Geophys. Res., **103**, 27637–27653.

Jacobs, S.S., Amos, A.F. and Bruchhausen, P.M. (1970): Ross Sea oceanography and Antarctic Bottom Water formation. Deep-Sea Res., **17**, 935–962.

Klatt, O., Roether, W., Hoppema, M., Bulsiewicz, K., Fleischmann, U., Rodehacke, C., Fahrbach, E., Weiss, R.F. and Bullister, J.L. (2002): Repeated CFC sections at the Greenwich Meridian in the Weddell Sea. J. Geophys. Res., **107**, C4, 10.1029/2000JC000731.

Locarnini, R.A., Whiteworth, III, T. and Nowlin, W.D., Jr. (1993): The importance of the Scotia Sea on the outflow of Weddell Sea Deep Water. J. Mar. Res., **51**, 135–153.

Masumoto, Y., Sasaki, H., Kagimoto, T., Komori, N., Ishida, A., Sasai, Y., Miyama, T., Motoi, T., Mitsudera, H., Takahashi, K., Sakuma, H. and Yamagata, T. (2004): A fifty-year-eddy-resolving simulation of the world ocean: Preliminary outcomes of OFES (OGCM for the Earth Simulator). J. Earth Simulator, **1**, 35–56.

Orsi, A.H., Johnson, G.C. and Bullister, J.L. (1999): Circulation, mixing, and production of Antarctic Bottom Water. Prog. Oceanogr., **43**, 55–109.

Pacanowski, R.C. and Griffies, S.M. (2000): MOM 3.0 Manual. Geophysical Fluid Dynamics Laboratory/National Oceanic and Atmospheric Administration, 680 p.

Rintoul, S.R. and Bullister, J.L. (1999): A late winter hydrographic section from Tasmania to Antarctica. Deep-Sea Res., I, **46**, 1417–1454.

Rosati, A. and Miyakoda, K. (1988): A general circulation model for upper ocean circulation. J. Phys. Oceanogr., **18**, 1601–1626.

Sasai, Y., Ishida, A., Yamanaka, Y. and Sasaki, H. (2004): Chlorofluorocarbons in a global ocean eddy-resolving OGCM: Pathway and formation of Antarctic Bottom Water. Geophys. Res. Lett., **31**, L12305, doi: 10.1029/2004GL019895.

Sen Gupta, A. and England, M.H. (2004): Evaluation of interior circulation in a high-resolution global ocean

model. Part I: Deep and Bottom waters. J. Phys. Oceanogr., **34**, 2592–2614.
Smethie, W.M., Jr., Fine, R.A., Putzka, A. and Jones, E.P. (2000): Tracing the flow of North Atlantic Deep Water using chlorofluorocarbons. J. Geophys. Res., **105**, 14297–14323.
Walker, S.J., Weiss, R.F. and Salameh, P.K. (2000): Reconstructed histories of the annual mean atmospheric mole fractions for halocarbons CFC-11, CFC-12, CFC-113, and carbon tetrachloride. J. Geophys. Res., **105**, 14285–14296.
Walsh, J. (1978): A dataset on northern hemisphere sea ice extent, 1953–1976. Rep. Glaciological Data No. GD-2, World Data Center for Glaciology, 49–51.
Wanninkof, R. (1992): Relationship between wind speed and gas exchange over the ocean. J. Geophys. Res., **97**, 7373–7382.
Warner, M.J. and Weiss, R.F. (1985): Solubilities of chlorofluorocarbons 11 and 12 in water and sea water. Deep-Sea Res., **32**, 1485–1497.
Warner, M.J. and Weiss, R.F. (1992): Chlorofluoromethanes in the South Atlantic Antarctic Intermediate Water. Deep-Sea Res., **39**, 2053–2075.
Watanabe, Y.W., Harada, K. and Ishikawa, K. (1994): Chlorofluorocarbons in the central North Pacific and southward spreading time of North Pacific intermediate water. J. Geophys. Res., **99**, 25195–25213.
Whitworth, T., III, Nowlin, W.D., Jr., Orsi, A.H., Locarnini, R.A. and Smith, S.G. (1994): Weddell sea shelf water in the Bransfield strait and Weddell-Scotia Confluence. Deep-Sea Res. I, **41**, 629–641.
WOCE (World Ocean Circulation Experiment) Data Products Committee (2000): WOCE Global Data, Version 2.0. -WOCE International Program Office, WOCE Report No 171/00, Southampton, U.K.
Zwally, H.J., Comiso, J., Parkinson, C., Campbell, W., Carsey, F. and Gloerson, P. (1983): Antarctic Sea Ice, 1973–1976: Satellite Passive Microwave Observations. NASA SP-459, NASA Scientific and Technical Information Program, 206 p.